Forefoot Pain Involving the Metatarsal Region: Differential Diagnosis with MR Imaging[1]

Carol J. Ashman, MD • Rosemary J. Klecker, MD • Joseph S. Yu, MD

CME FEATURE

See accompanying test at http://www.rsna.org/education/rg_cme.html

LEARNING OBJECTIVES FOR TEST 3

After reading this article and taking the test, the reader will be able to:

- Describe the MR imaging features of common bone lesions and joint processes that can produce pain in the metatarsal region of the forefoot.
- List the MR imaging features of soft-tissue disorders that produce forefoot pain proximal to the toes.
- Formulate a differential diagnosis of soft-tissue masses of the metatarsal region.

Many disorders produce discomfort in the metatarsal region of the forefoot. These disorders include traumatic lesions of the soft tissues and bones (eg, turf toe, plantar plate disruption, sesamoiditis, stress fracture, stress response), Freiberg infraction, infection, arthritis, tendon disorders (eg, tendinosis, tenosynovitis, tendon rupture), nonneoplastic soft-tissue masses (eg, ganglia, bursitis, granuloma, Morton neuroma), and, less frequently, soft-tissue and bone neoplasms. Prior to the advent of magnetic resonance (MR) imaging, many of these disorders were not diagnosed noninvasively, and radiologic involvement in the evaluation of affected patients was limited. However, MR imaging has proved useful in detecting the numerous soft-tissue and early bone and joint processes that occur in this portion of the foot but are not depicted or as well characterized with other imaging modalities. Frequently, MR imaging allows a specific diagnosis based on the location, signal intensity characteristics, and morphologic features of the abnormality. Consequently, MR imaging is increasingly being used to evaluate patients with forefoot complaints. Radiologists should be familiar with the differential diagnosis and MR imaging features of disorders that can produce discomfort in this region.

Abbreviations: MTP = metatarsophalangeal, STIR = short-inversion-time inversion recovery

Index terms: Arthritis, 465.70 • Foot, fractures, 465.415 • Foot, infection, 465.21 • Foot, MR, 465.1214, 465.121413 • Foot, neoplasms, 465.30 Joints, diseases, 465.70 • Joints, MR, 465.1214

RadioGraphics 2001; 21:1425–1440

[1]From the Department of Radiology, Ohio State University Medical Center, S209 Rhodes Hall, Columbus, OH 43210. Presented as an education exhibit at the 2000 RSNA scientific assembly. Received March 16, 2001; revision requested April 3 and received June 19; accepted July 10. **Address correspondence to** C.J.A. (e-mail: *cajaas@yahoo.com*).

Figure 1. **(a–c)** Turf toe in a 24-year-old professional football player who sustained an acute hyperextension injury at the first MTP joint. **(a)** Sagittal T1-weighted MR image shows a disrupted plantar plate (arrow) between the sesamoid bone and the base of the proximal phalanx of the great toe. **(b)** Sagittal short-inversion-time inversion recovery (STIR) MR image demonstrates edema in the region of the plantar plate (arrow). **(c)** Sagittal STIR MR image obtained adjacent to **b** demonstrates subchondral bone marrow edema (short arrow) and surface irregularity of the first metatarsal head (long arrow). **(d)** Intact plantar plate in an asymptomatic 30-year-old woman. Sagittal fat-suppressed fast spin-echo proton-density–weighted MR image shows the plantar plate (long arrow) as a low-signal-intensity band dorsal to the flexor tendons (short arrow).

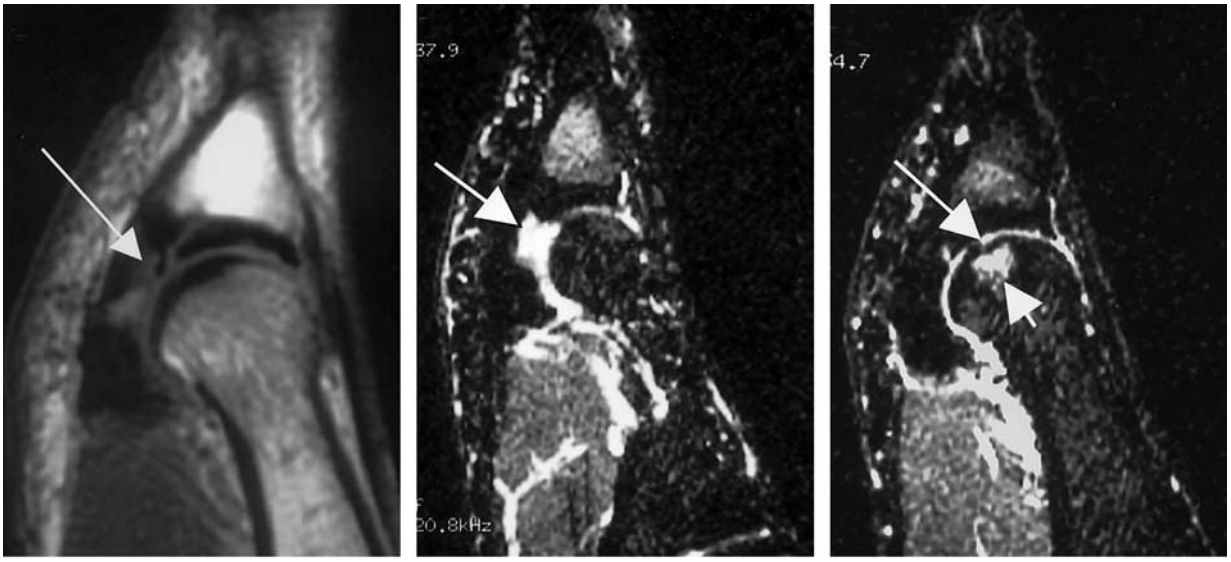

a. b. c.

d.

Introduction

Forefoot pain is a common clinical problem. Numerous disease processes produce pain in the region of the metatarsal bones, and the cause may be difficult to establish based solely on clinical findings. Although conventional radiography is useful in detecting bone lesions, it typically does not allow diagnosis of early bone abnormalities or soft-tissue disorders producing forefoot pain. Magnetic resonance (MR) imaging, with its excellent soft-tissue contrast and multiplanar imaging capability, plays an important role in the evaluation of patients with discomfort in this region of the foot. Often, a specific diagnosis is revealed only at MR imaging.

In this article, we review the MR imaging appearances of disorders that are capable of producing pain in the forefoot proximal to the phalanges. These disorders include trauma-related conditions, Freiberg infraction, infection, joint disorders, tendon disorders, nonneoplastic soft-tissue masses, soft-tissue neoplasms, and bone neoplasms.

Trauma

Turf Toe

Turf toe most commonly occurs in football players who play on hard, artificial surfaces and wear lightweight, flexible shoes. Hyperextension injury at the first metatarsophalangeal (MTP) joint may result in partial or complete disruption of the fibrocartilaginous plantar plate, a structure that extends from the volar aspect of the metatarsal necks to the proximal phalanges of the toes and reinforces the MTP joint capsule (Fig 1) (1,2). Plantar plate rupture manifests as discontinuity of the structure, along with increased signal intensity in the soft tissues plantar to the sesamoid bones

Figure 2. Disrupted plantar plate at the second MTP joint in a 48-year-old woman who presented with foot pain. The patient had no history of acute trauma. **(a)** Coronal fat-suppressed fast spin-echo proton-density–weighted MR image shows edema in the region of the plantar plate. The lateral aspect of the plate is not visualized (arrow). **(b, c)** Sagittal gadolinium-enhanced fat-suppressed T1-weighted MR images obtained at the medial **(b)** and lateral **(c)** aspects of the second MTP joint show a thin, irregular, indistinct plantar plate medially (arrows in **b**). The plate appears to be disrupted laterally (arrow in **c**). Note the fluid accumulation and contrast material enhancement within the joint and the adjacent flexor tendon sheath, findings that indicate synovitis and tenosynovitis, respectively. The proximal phalanx is hyperextended.

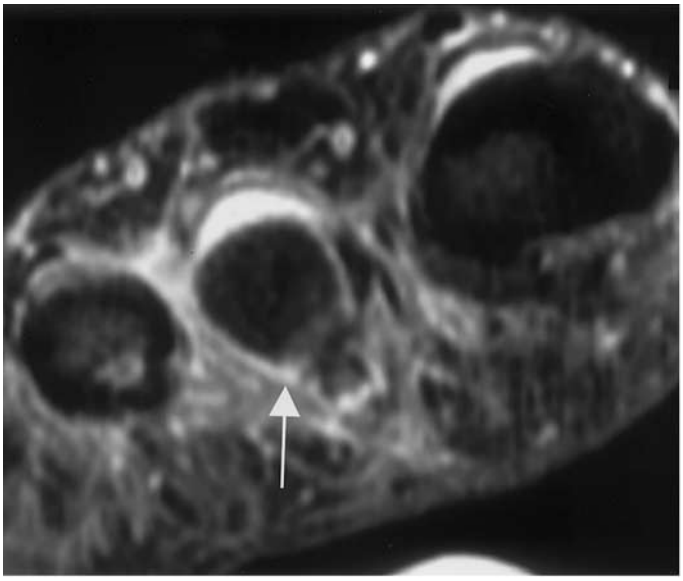

a.

b.

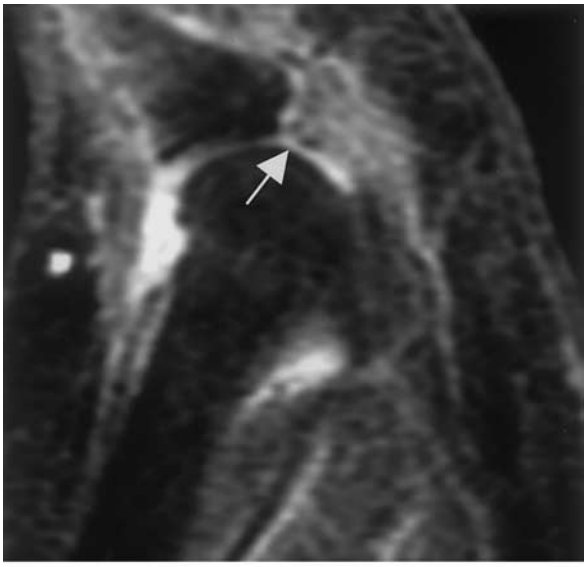

c.

on STIR MR images (3) and increased signal intensity on T2-weighted images (4). Concomitant injury to the articular cartilage and subchondral bone may also occur (1).

Plantar Plate Disruption

Plantar plate disruption at the second through fifth MTP joints occurs more frequently in women. The increased weight-bearing load and hyperextension forces placed on the MTP joint by high-heeled, pointed shoes (5) are likely predisposing factors. The second MTP joint is most commonly affected. MR imaging findings include increased signal intensity in and around the plantar plate on T2-weighted images, discontinuity of the plate, MTP joint synovitis, flexor tendon sheath synovitis, and persistent hyperextension of the proximal phalanx (Fig 2) (2).

Sesamoiditis

Sesamoiditis is a painful inflammatory condition produced by repetitive injury to the plantar aspect of the forefoot (6). MR imaging findings in the marrow of the sesamoid bones include decreased or normal signal intensity on T1-weighted images and increased signal intensity on STIR images (Fig 3). The bone signal intensity changes are similar to those caused by a stress response, and there may be some overlap between these conditions. If the signal intensity of the sesamoid bones is abnormal on STIR MR images but normal on T1-weighted images, sesamoiditis is a more probable diagnosis than a stress response. Involvement of both sesamoid bones also favors a diagnosis of sesamoiditis. Reactive soft-tissue abnormalities including tendinitis, synovitis, and bursitis are characteristic findings in sesamoiditis and are useful differentiating features (3).

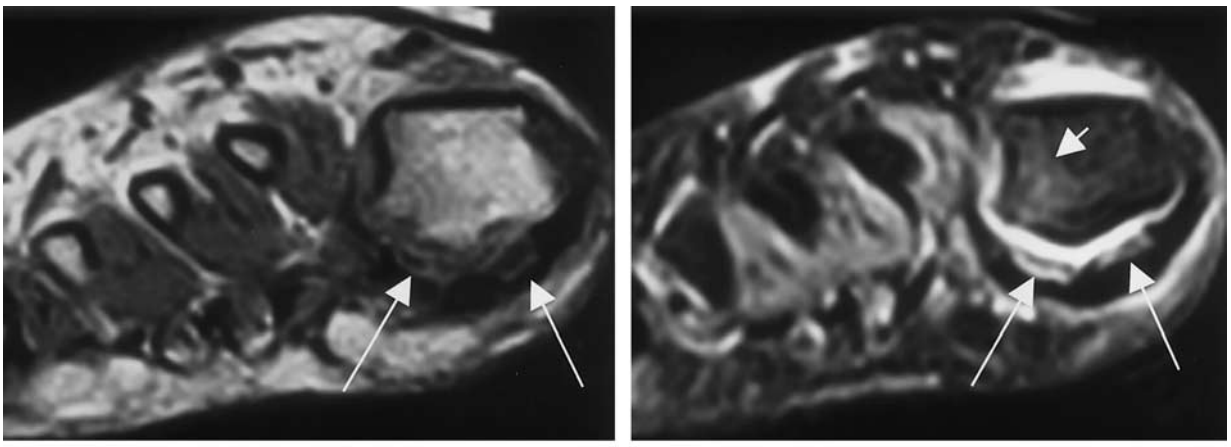

a. b.

Figure 3. Sesamoiditis in a 21-year-old female kickboxer. **(a)** Coronal T1-weighted MR image shows the tibial and fibular sesamoid bones with low signal intensity (arrows). **(b)** Corresponding coronal STIR MR image shows the sesamoid bones with increased signal intensity (long arrows). Note the adjacent soft-tissue edema and joint effusion. Involvement of both sesamoid bones, joint effusion, and inflammatory changes in the adjacent soft tissues favor a diagnosis of sesamoiditis rather than stress response. However, the small amount of bone marrow edema within the first metatarsal head (short arrow) probably represents a stress response.

Stress Fractures

Stress fractures in the metatarsal bones are common in runners, ballet dancers, gymnasts, and military recruits (7). Conditions resulting in altered weight bearing , including a hallux valgus deformity, recent surgery of the hallux, and a low longitudinal arch of the foot, increase the risk of developing a stress fracture. The middle or distal portions of the second, third, or fourth metatarsal shafts are most often involved. Stress injuries may also occur in the sesamoid bones of the hallux and at the synchondrosis between the portions of a bipartite sesamoid bone (6). Subchondral fractures may occur in the metatarsal head in diabetic patients with neuropathic arthropathy; these fractures may appear identical to a stress fracture (8).

Stress Response

A stress response manifests as an amorphous area of decreased signal intensity within the marrow on T1-weighted MR images that increases in signal intensity on corresponding T2-weighted and STIR images. Edema may be present in the adjacent soft tissues, and contrast enhancement may occur following intravenous administration of gadopentetate dimeglumine. These findings are nonspecific, and correlation with clinical findings is essential for making a correct diagnosis. A stress response may progress to a stress fracture, which is characterized by a band of low signal intensity contiguous with the cortex on both T1- and T2-weighted images (Fig 4) (9–11).

Radiographically Occult Fractures

Radiographically occult fractures can be accurately detected with MR imaging. The fracture line appears as a linear abnormality with low signal intensity on T1-weighted images. Marrow with low signal intensity on T1-weighted images and high signal intensity on corresponding T2-weighted and STIR images surrounds the fracture (4). MR imaging is particularly useful in detecting occult fractures in osteopenic patients.

Freiberg Infraction

Freiberg infraction is a disorder affecting the metatarsal head (usually the second or third metatarsal head) and is characterized at pathologic analysis by collapse of the subchondral bone, osteonecrosis, and cartilaginous fissures. The cause of Freiberg infraction is controversial and is probably multifactorial. A traumatic insult in the form of either acute or repetitive injury and vascular compromise are the most popular theories. Freiberg infraction is more common in women and most commonly manifests during adolescence. High-heeled shoes have been implicated as a causative factor (12). Patients may present with pain and limited motion, although symptoms may not begin until degenerative arthrosis has developed.

Early MR imaging findings include low-signal-intensity changes in the metatarsal head on T1-weighted images with increased signal intensity on corresponding T2-weighted and STIR images (4). These changes are nonspecific and may also

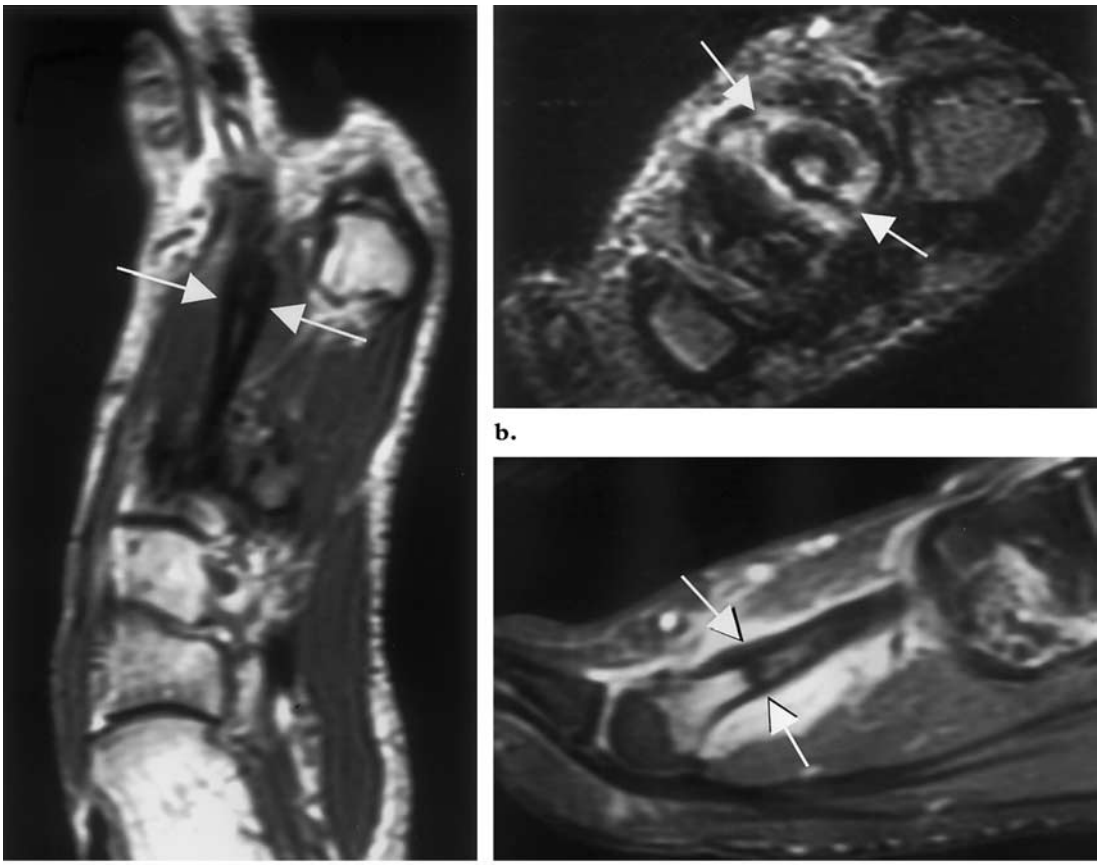

Figure 4. Stress fracture of the second metatarsal shaft in a 19-year-old male runner. The patient had no history of acute trauma. **(a)** Axial T1-weighted MR image shows cortical thickening, a low-signal-intensity horizontal band representing a fracture line spanning the width of the bone (arrows), and adjacent low-signal-intensity changes within the marrow. **(b)** Coronal T2-weighted MR image shows increased signal intensity within the marrow and adjacent soft tissues (arrows). **(c)** On a gadolinium-enhanced fat-suppressed T1-weighted MR image, the fracture line is more conspicuous (arrows). Note the intense contrast enhancement of the adjacent bone marrow and soft tissues.

be seen in a stress response of the metatarsal head. There may in fact be overlap between these conditions (8). With disease progression, flattening of the metatarsal head occurs, and low-signal-intensity changes develop on T2-weighted images as the bone becomes sclerotic.

Infection

Osteomyelitis

Osteomyelitis of the foot most often results from transcutaneous spread of infection and most commonly occurs in diabetic patients (13). Cutaneous ulcers may develop at pressure points, especially under the first and fifth metatarsal heads (14). When ulcerations become infected, contiguous spread to the underlying metatarsal head and MTP joint may occur.

MR imaging findings in osteomyelitis include low signal intensity within the infected bone marrow on T1-weighted images, increased signal intensity on T2-weighted and STIR images, and contrast enhancement following intravenous administration of gadopentetate dimeglumine (Fig 5) (13,15). Secondary signs of osteomyelitis may help distinguish between osteomyelitis and acute neuropathic disease, which demonstrates similar imaging findings (13). These secondary signs include a cutaneous ulcer, cellulitis, phlegmon, soft-tissue abscess (Fig 6), sinus tract, and cortical interruption.

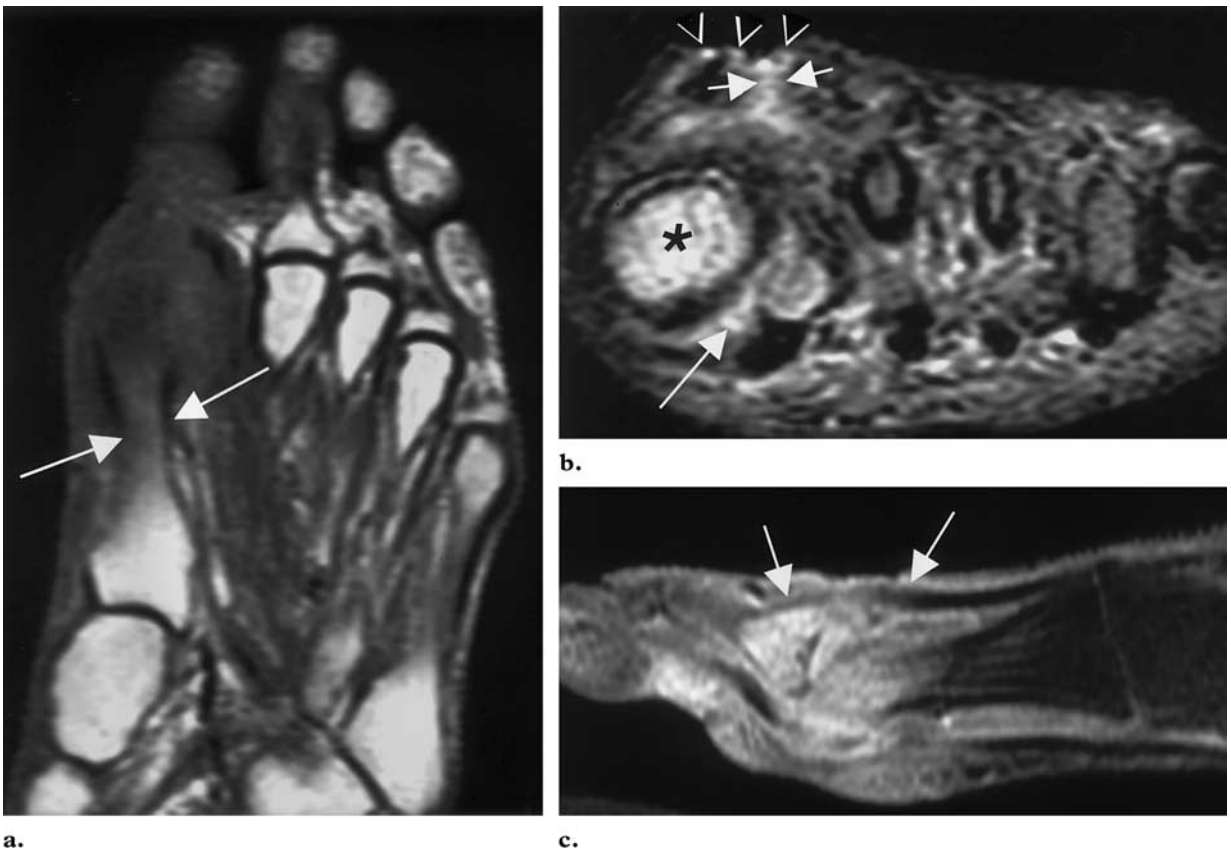

Figure 5. Osteomyelitis of the first metatarsal head and septic arthritis of the first MTP joint in a 30-year-old woman with systemic lupus erythematosus. **(a)** Axial T1-weighted MR image shows an area of diffuse low signal intensity within the marrow of the distal first metatarsal bone (arrows). Similar changes were also present within the base of the proximal phalanx of the great toe. **(b)** Coronal T2-weighted MR image demonstrates a dorsal cutaneous ulcer (arrowheads), dorsal sinus tract (short arrows), high-signal-intensity changes in the soft tissues representing cellulitis, increased signal intensity within the marrow of the metatarsal head (*), and joint effusion (long arrow). **(c)** Sagittal fat-suppressed T1-weighted MR image reveals intense contrast enhancement of the bone marrow, joint, and soft tissues. Note that the extensor tendon sheath dorsal to the first ray demonstrates both edema and enhancement (arrows), findings that indicate tenosynovitis.

Septic Arthritis

Septic arthritis of the MTP joints is also most commonly seen in diabetic patients and is caused by the spread of infection from an adjacent soft-tissue or bone source (Fig 5) (16). MR imaging findings include increased joint fluid and synovial thickening and enhancement (4,16,17). Marrow signal intensity changes and enhancement in the subarticular bone are similar to those seen in osteomyelitis. These findings are nonspecific and may also be seen in acute neuropathic disease and inflammatory arthritis. Soft-tissue signs of infection support the diagnosis of septic arthritis.

Joint Disorders

Neuropathic Osteoarthropathy

Neuropathic osteoarthropathy is a common complication of diabetes mellitus (14,18). The intertarsal and tarsometatarsal joints are most com-

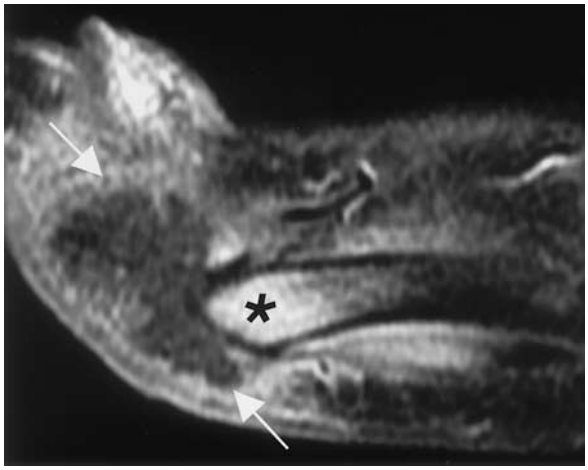

Figure 6. Osteomyelitis in a 25-year-old diabetic man with burning foot pain. Sagittal gadolinium-enhanced fat-suppressed T1-weighted MR image demonstrates a low-signal-intensity fluid collection with peripheral enhancement representing an abscess plantar to the fifth metatarsal head (arrows). Note also the intense enhancement of the adjacent fifth metatarsal bone (*), a finding that indicates osteomyelitis.

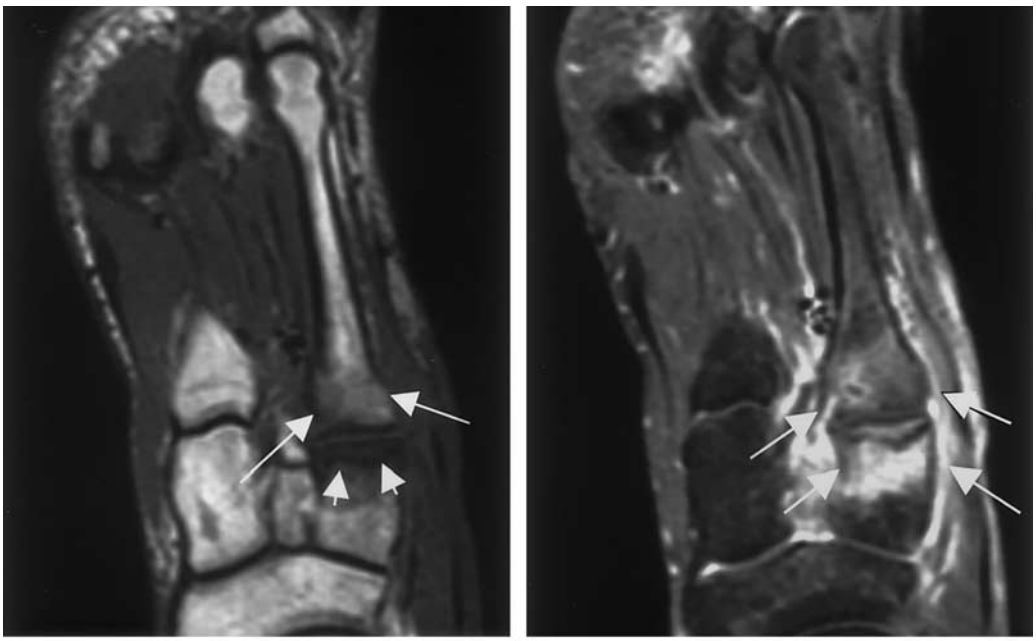

a. b.

Figure 7. Early neuropathic osteoarthropathy in a 49-year-old diabetic man who complained of foot pain and swelling. The patient had no history of trauma or unusual activity. **(a)** Axial T1-weighted MR image shows a serpentine band of low signal intensity in the lateral cuneiform bone representing a subchondral fracture (short arrows). Adjacent low-signal-intensity bone marrow edema is also present within the proximal third metatarsal bone (long arrows). **(b)** Axial gadolinium-enhanced fat-suppressed T1-weighted MR image shows contrast enhancement of periarticular bone (arrows) and adjacent soft tissues.

monly involved, followed by the MTP joints. Impaired pain sensation and proprioception lead to repetitive trauma and joint destabilization. Arteriovenous shunting and sympathetic nerve dysfunction produce increased blood flow and osteolysis. Joint misalignment, disorganization, and destruction and bone fragmentation are characteristic pathologic features. Although patients have impaired sensation, the disease may be painful in its acute stage.

Early MR imaging features include decreased signal intensity in the juxta-articular bone on T1-weighted images and increased signal intensity on T2-weighted and STIR images (Fig 7). Contrast enhancement may occur after intravenous administration of gadopentetate dimeglumine. The adjacent soft tissues are edematous. Acutely, these findings are nonspecific and similar to those produced by osteomyelitis, which may coexist with neuropathic disease (14,18). Skin ulcers, sinus tracts, and abscess formation adjacent to areas of abnormal bone signal intensity support the diagnosis of osteomyelitis. In difficult cases, biopsy may be the only means of excluding infection. Chronic changes in neuropathic osteoarthropathy include periarticular cyst formation, bone fragmentation, joint misalignment, joint effusion, and soft-tissue edema (15,18). Osteosclerosis demonstrates subchondral low signal intensity on T1- and T2-weighted MR images. The signal intensity of juxta-articular bone is variable on T2-weighted images, however, and high-signal-intensity changes may be present (19,20).

Osteoarthritis

Osteoarthritis is a common finding in the first MTP joint and is most often produced by repetitive loading injury (21). Resultant painful limitation of motion is referred to as hallux rigidus (22). Osteoarthritis of the hallucal sesamoid articulations is also common. A hallux valgus deformity may precipitate degenerative changes in the first ray.

Joint space narrowing, marginal osteophytes, subchondral cyst formation, ossicle formation, subchondral marrow edema (which demonstrates low signal intensity on T1-weighted images and increased signal intensity on T2-weighted and STIR images), and subchondral sclerosis (with decreased signal intensity on both T1- and T2-weighted images) are characteristic MR imaging findings in osteoarthritis (Fig 8) (23).

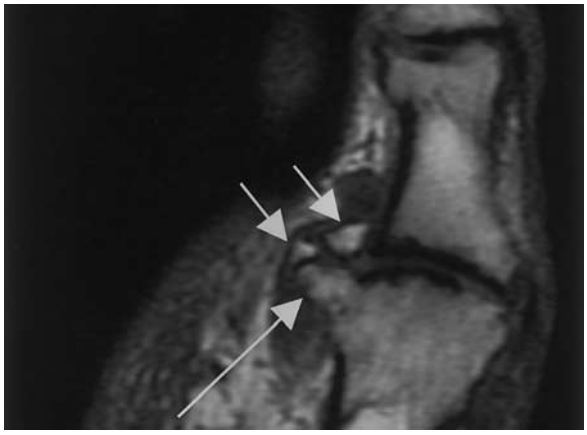

Figure 8. Osteoarthritis at the first MTP joint in a 50-year-old man. Axial T1-weighted MR image shows a large marginal osteophyte (long arrow), ossicles at the lateral joint margin (short arrows), medial joint space narrowing, and subchondral low signal intensity within the first metatarsal head and proximal phalanx of the great toe.

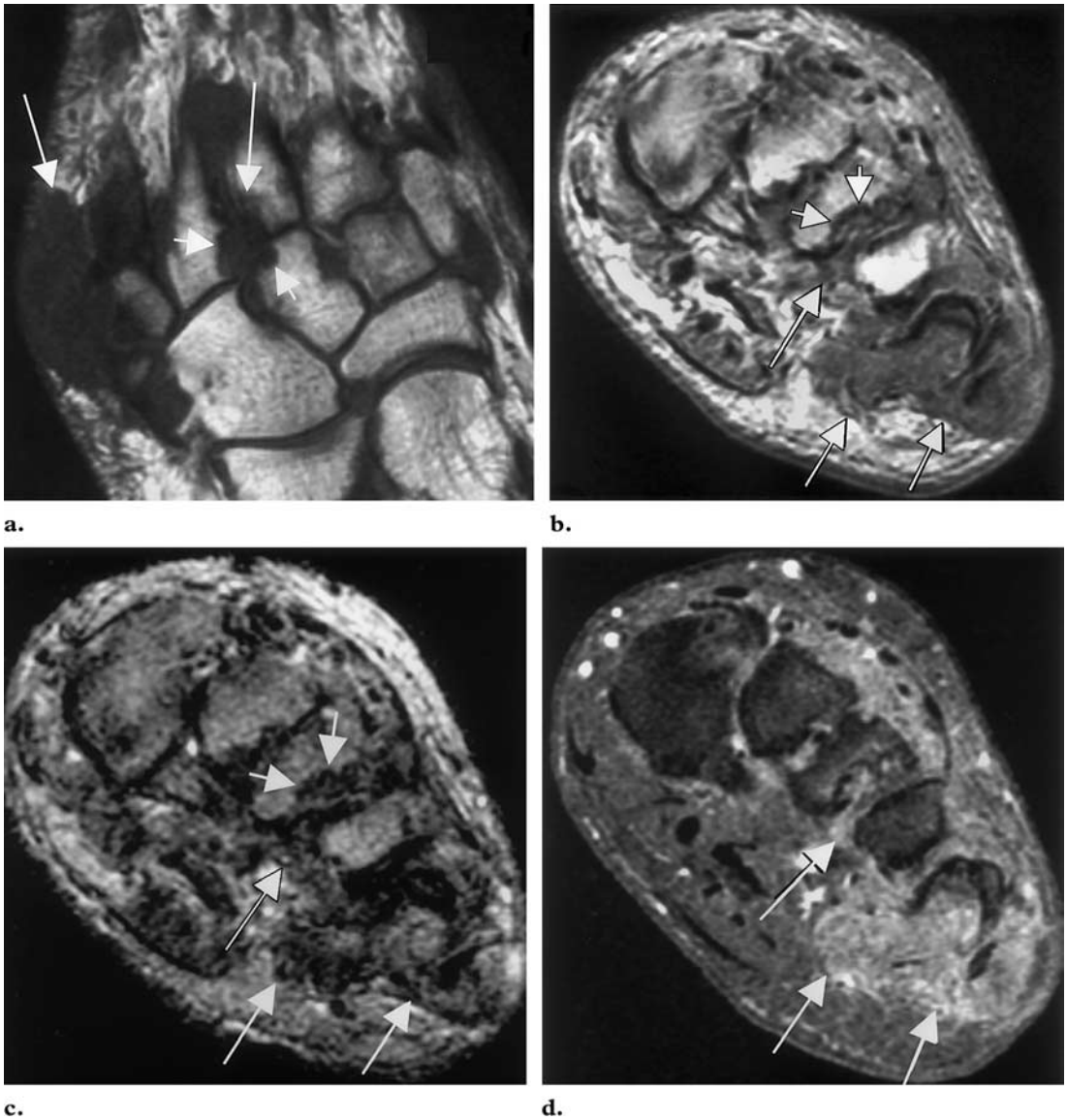

Figure 9. Tophaceous gout involving the intermetatarsal and tarsometatarsal region of the foot in a 56-year-old man with hyperuricemia who presented with foot pain and swelling. **(a)** Axial T1-weighted MR image shows low-signal-intensity tophi (long arrows) and adjacent periarticular erosions with characteristic overhanging edges (short arrows). The joint spaces are preserved, as is typical in gout. **(b, c)** Coronal proton-density–weighted **(b)** and T2-weighted **(c)** MR images obtained at the level of the tarsometatarsal joint reveal erosions (short arrows) and low-signal-intensity tophi (long arrows). (Fig 9b and 9c reprinted, with permission, from reference 24.) **(d)** Gadolinium-enhanced fat-suppressed T1-weighted MR image shows increased contrast enhancement of the tophi (arrows) and juxta-articular bone.

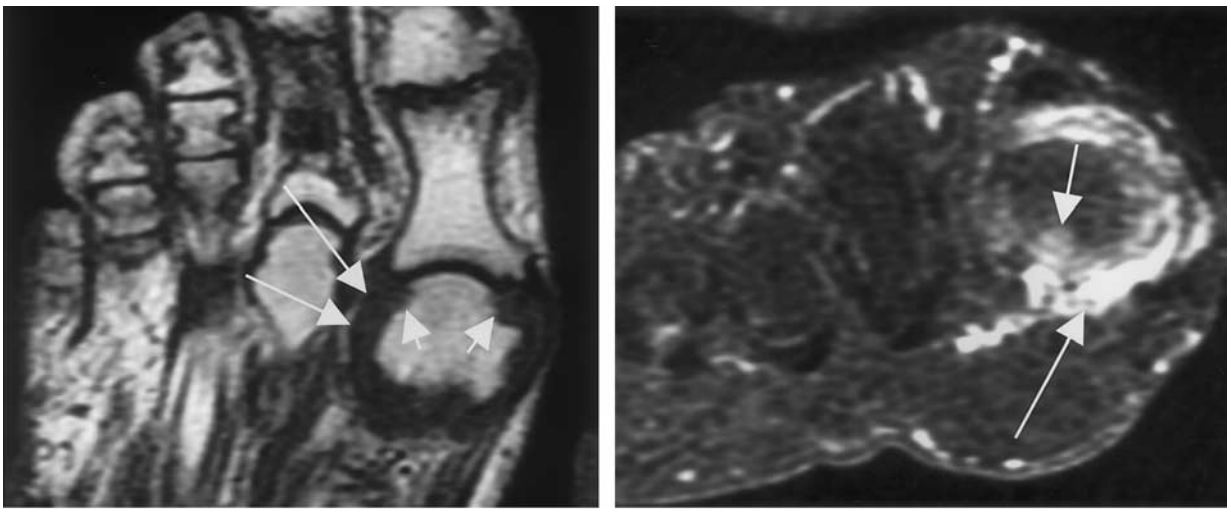

a. b.

Figure 10. Rheumatoid arthritis in a 71-year-old woman with pain at the first MTP joint. **(a)** Axial T1-weighted MR image shows marginal erosions at the first metatarsal head (short arrows), low-signal-intensity synovial thickening (long arrows), and joint space narrowing. Note also the erosive changes at the interphalangeal joint of the great toe. **(b)** Coronal gadolinium-enhanced fat-suppressed T1-weighted MR image shows contrast enhancement of the synovium (long arrow) and subchondral bone (short arrow). The signal intensity changes in both **a** and **b** are nonspecific; however, a previously established diagnosis of rheumatoid arthritis in the hands, a lack of clinical indicators of infection, a normal serum urate level, and a positive response to steroids supported the diagnosis of rheumatoid arthritis at the first MTP and interphalangeal joints.

Gout

Gout is caused by the deposition of sodium urate crystals in joints, bones, tendons, bursae, and periarticular tissue. It most commonly affects the first MTP joint, and monoarticular involvement is typical. The MR imaging features of acute gout are nonspecific and include joint effusion and synovial thickening (17). Tophaceous gout represents the chronic form of the disease. Tophi may produce bone erosions and occur at intra-articular or periarticular locations or at a distance from a joint, manifesting as a soft-tissue mass. Tophi have intermediate to low signal intensity on T1-weighted MR images. Their signal intensity is variable on T2-weighted images, but heterogeneous low signal intensity should prompt consideration of this entity (Fig 9). Contrast enhancement often occurs after administration of gadopentetate dimeglumine, particularly in acutely symptomatic patients (24). Tophaceous gout may be confused with rheumatoid arthritis, septic arthritis, or even a neoplastic process at MR imaging; correlation with the clinical presentation and serum urate level is necessary in these situations.

Rheumatoid Arthritis

Rheumatoid arthritis commonly affects the feet. The earliest changes occur at the MTP joints (25). Pannus is inflammatory synovial tissue and demonstrates low to intermediate signal intensity on T1-weighted MR images (Fig 10). Signal intensity may vary on T2-weighted images. High signal intensity indicates hypervascular pannus. With disease chronicity, fibrous pannus develops and hemosiderin deposition may occur, demonstrating low signal intensity on T2-weighted images. Additional findings include marginal erosions adjacent to the pannus, cartilage thinning, subchondral cysts and marrow edema, joint effusion, tenosynovitis, and bursitis. Enhancement of pannus can be seen immediately after contrast material administration (26–28).

Tendon Disorders

Tendinosis

Tendinosis is characterized by angiofibroblastic hyperplasia, degeneration, and necrosis of the involved tendon with few or no inflammatory cells (29). On T1- and proton-density–weighted MR images, there is an area of increased signal intensity and either fusiform or diffuse tendon thickening. The areas of increased signal intensity persist on T2-weighted images if significant degeneration is present (30).

Tenosynovitis

Tenosynovitis is inflammation of the tendon sheath and may be due to synovial inflammatory disease, infection (Fig 5), or mechanical irritation.

Fluid accumulates in the sheath, and contrast enhancement of the sheath typically occurs following intravenous administration of gadopentetate dimeglumine. Tenosynovitis may affect the flexor hallucis longus tendon between the sesamoid bones, where it is subject to repetitive impact, and under the base of the first metatarsal bone, where the flexor digitorum longus crosses under the flexor hallucis longus (31,32). Stenosing tenosynovitis is caused by chronic inflammation, leading to fibrosis and tendon entrapment. Tendon degeneration and rupture may also result. Reported MR imaging findings in stenosing tenosynovitis include thickening of the tendon or tendon sheath, increased fluid within the tendon sheath, and enhancement of the tendon sheath following intravenous administration of gadopentetate dimeglumine (33–35).

Tendon Ruptures

Tendon ruptures occur in tendons weakened by degeneration, repetitive microtrauma, infection, or systemic disease such as diabetes. Rupture of a normal tendon is caused by laceration or sudden force, creating discontinuity of the tendon fibers and intervening edema on T2-weighted MR images (Fig 11) (36). Partial ruptures demonstrate increased signal intensity within the tendon substance on T1-, proton-density–, and, occasionally, T2-weighted images (Fig 12) (30).

Nonneoplastic Soft-Tissue Masses

The vast majority of soft-tissue masses of the foot are nonneoplastic. Inflammatory lesions such as bursitis and foreign body granulomas are usually painful. Noninflammatory masses may cause pain as a result of mass effect or compression of adjacent structures (37,38).

Ganglia

Ganglia are the most common soft-tissue masses of the foot and ankle. In the forefoot, a ganglion is typically located dorsal to the MTP joints and tendons. Ganglia are thought to be a result of repetitive trauma leading to mucoid cystic degeneration (39). A ganglion manifests as a well-defined mass with low to intermediate signal intensity on T1-weighted MR images depending on its protein content. Homogeneous high signal intensity is characteristic on T2-weighted and STIR images (Fig 13). Thin, peripheral rim enhancement may occur following intravenous administration of gadopentetate dimeglumine (40).

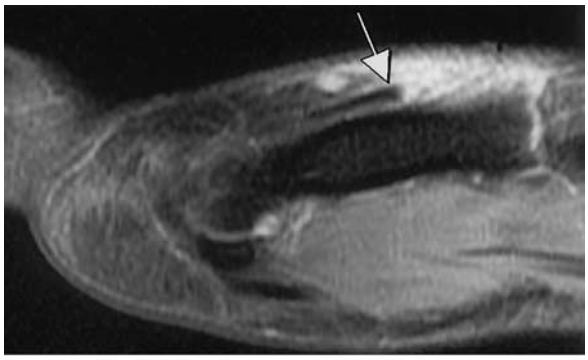

a.

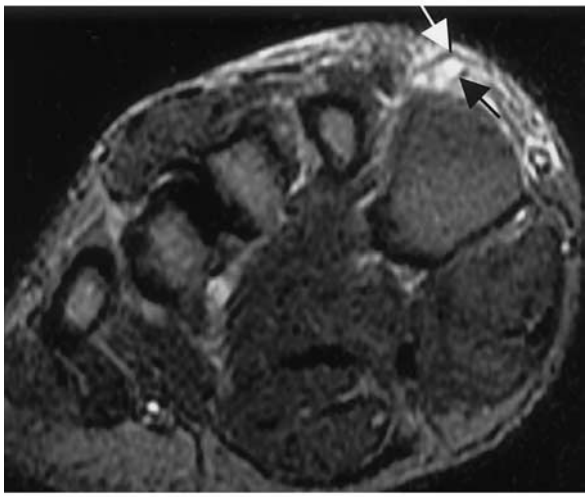

b.

Figure 11. Tendon rupture due to laceration of the dorsum of the foot in a 25-year-old woman with inability to dorsiflex the great toe. **(a)** Sagittal fat-suppressed fast spin-echo proton-density–weighted MR image shows complete rupture of the extensor hallucis longus tendon (arrow). **(b)** Coronal T2-weighted MR image shows a fluid-filled gap at the expected location of the tendon at the level of the proximal first metatarsal bone (arrows).

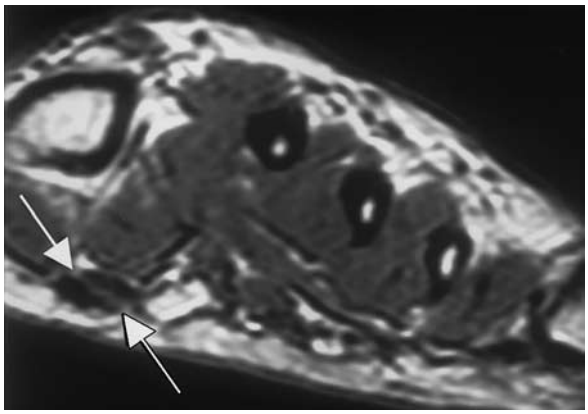

Figure 12. Partial tendon rupture in a 45-year-old male softball player. Coronal proton-density–weighted MR image reveals a partial longitudinal tear in the flexor hallucis longus tendon (arrows).

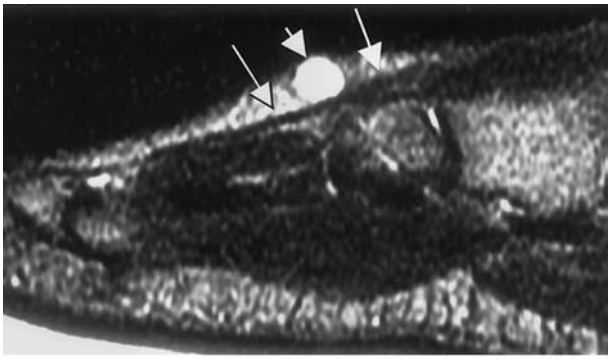

a.

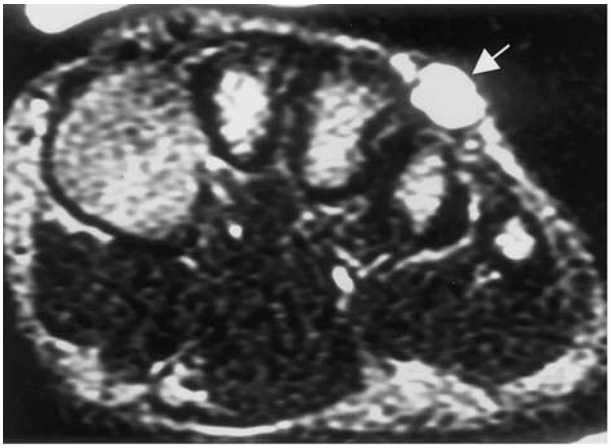

b.

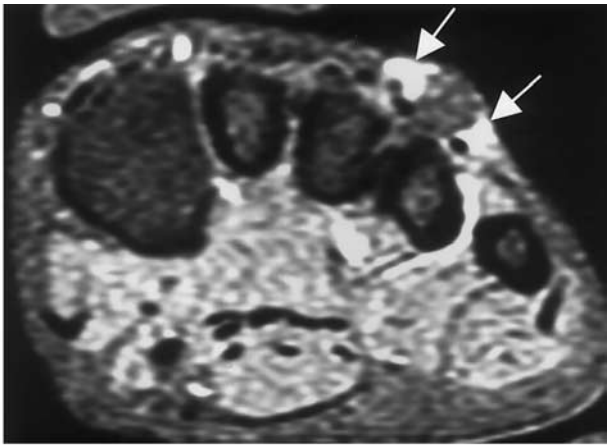

c.

Figure 13. Dorsal ganglion in a 25-year-old woman who presented with a painful soft-tissue mass. **(a, b)** Sagittal **(a)** and coronal **(b)** T2-weighted MR images reveal a well-defined mass with high signal intensity and a mildly lobulated contour (short arrow) adjacent to the fourth extensor tendon (long arrows in **a**). **(c)** On a coronal gadolinium-enhanced fat-suppressed T1-weighted MR image, the mass demonstrates low signal intensity with peripheral enhancement (arrows).

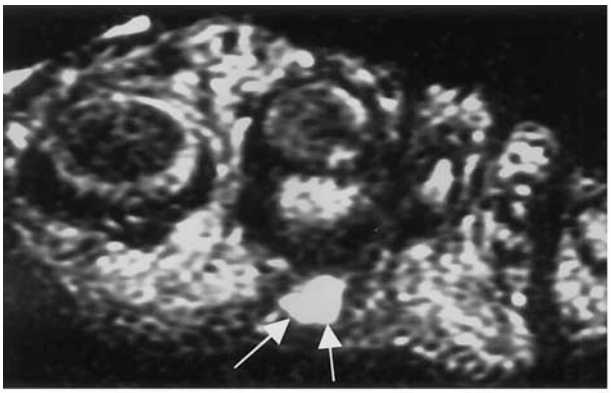

a.

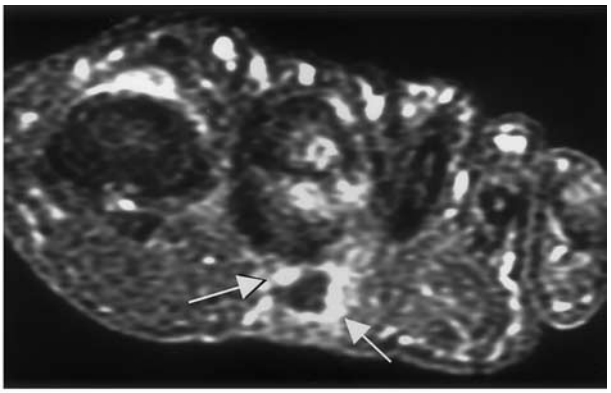

b.

Figure 14. Submetatarsal bursitis in a 60-year-old woman with pain under the second metatarsal head. **(a)** Coronal T2-weighted MR image shows a well-defined mass with high signal intensity (arrows). **(b)** On a coronal gadolinium-enhanced fat-suppressed T1-weighted MR image, the mass demonstrates low signal intensity with peripheral enhancement (arrows).

Bursitis

Bursitis can occur in the forefoot and may involve the intermetatarsal bursae or the adventitial bursae beneath the metatarsal heads (41,42). Trauma, infection, rheumatoid arthritis, and gout may all cause bursitis. The most important distinguishing feature of a bursa is its location. A well-defined fluid collection is seen at a pressure point and demonstrates low signal intensity on T1-weighted MR images and high signal intensity on T2-weighted and STIR images (Fig 14). Peripheral enhancement is seen following intravenous administration of gadopentetate dimeglumine. Small fluid collections with a transverse diameter of 3 mm or less in the first three intermetatarsal bursae may be physiologic (43).

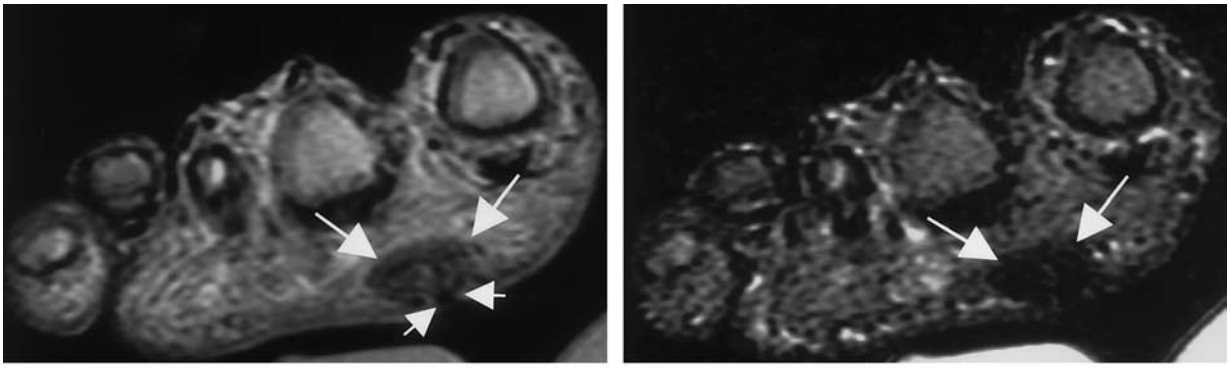

a. b.

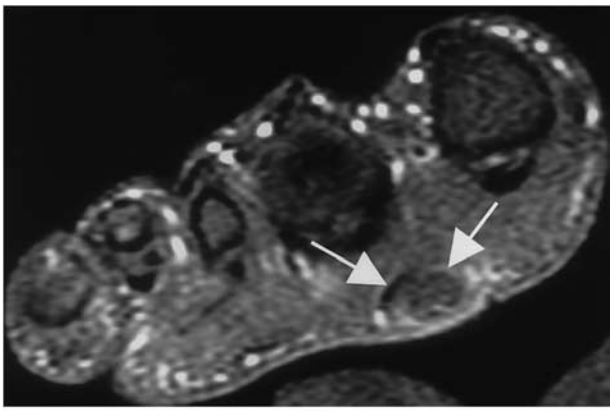

c.

Figure 15. Foreign body granuloma in a 26-year-old man. **(a)** Coronal proton-density–weighted MR image reveals a low-signal-intensity nodular lesion in the subcutaneous fat at the plantar aspect of the ball of the foot (long arrows). A channel communicating with the skin surface is also seen (short arrows). **(b)** On a coronal T2-weighted MR image, the lesion demonstrates low signal intensity (arrows). **(c)** Coronal gadolinium-enhanced fat-suppressed T1-weighted MR image shows the mass with peripheral enhancement (arrows), a finding that indicates inflammation.

Foreign Body Granulomas

Foreign body granulomas form in response to foreign objects such as thorns or pieces of wood, glass, or plastic that have penetrated the soft tissues of the foot (44). The lesion is a nonspecific mass with low signal intensity on T1-weighted MR images (Fig 15) and high signal intensity on T2-weighted images. The signal intensity pattern may be heterogeneous, and areas of low signal intensity corresponding to fibrosis may be present on T2-weighted images (45,46). In addition, peripheral contrast enhancement has been reported (47), and surrounding inflammation may be present (44). The foreign body can sometimes be visualized, demonstrating low signal intensity with all pulse sequences.

Calluses

Calluses may form in the subcutaneous fat adjacent to skin calluses, usually under the metatarsal heads. An area of low signal intensity on both T1- and T2-weighted MR images that enhances following intravenous administration of gadopentetate dimeglumine has been described (48).

Morton Neuromas

Morton neuromas are not true neoplasms; rather, they are masses composed of interdigital perineural fibrosis and nerve degeneration. Morton neuroma occurs between the metatarsal heads, most commonly between the third and fourth rays. The lesion is thought to arise as a result of compression of the interdigital nerve against the intermetatarsal ligament, although ischemia and compression of the nerve by an enlarged intermetatarsal bursa have also been suggested (49). Morton neuroma is more common in women, and high-heeled shoes have been implicated as a causative factor. Pain at the metatarsal head, often radiating to the toes, is characteristic (50). Morton neuroma is isointense to slightly hyperintense relative to muscle on T1-weighted MR images (Fig 16). It is iso- or hypointense relative to fat on T2-weighted images, resulting in poor lesion conspicuity. The use of gadopentetate dimeglumine is helpful because intense enhancement typically occurs on fat-suppressed T1-weighted images, increasing the conspicuity of the lesion (50,51).

Plantar Fibromatosis

Plantar fibromatosis consists of localized fibrous proliferation that arises from the superficial and medial aspect of the plantar fascia. One or more nodules may be present. Lesions have low to intermediate signal intensity on T1-weighted MR images and usually demonstrate low signal intensity on T2-weighted images (Fig 17). Contrast enhancement is variable (37,38).

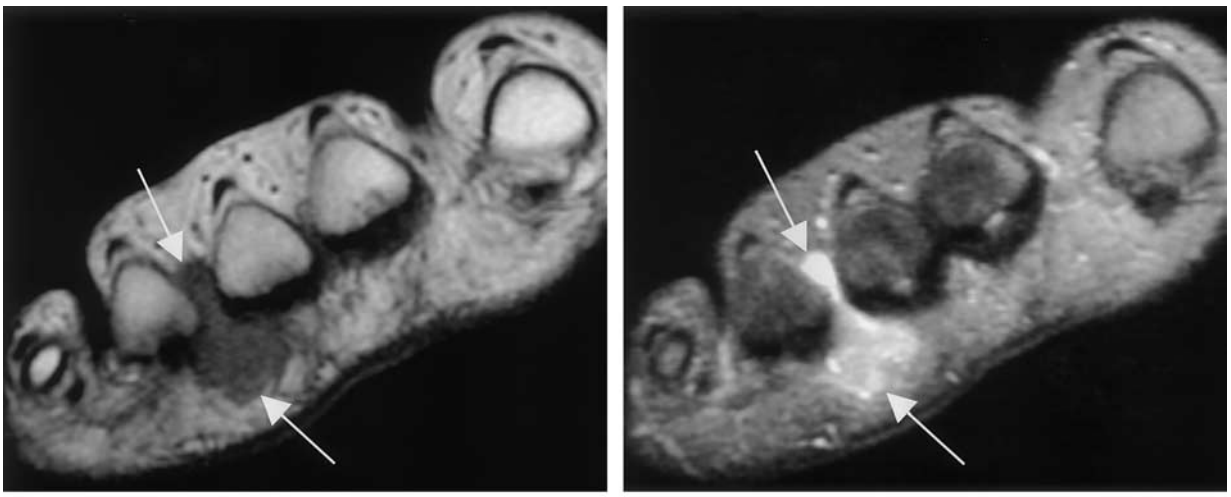

a. b.

Figure 16. Morton neuroma in a patient with pain at the level of the third MTP joint radiating into the toe. **(a)** Coronal T1-weighted MR image shows a large, teardrop-shaped mass with intermediate signal intensity at the third MTP interspace (arrows). **(b)** On a coronal gadolinium-enhanced fat-suppressed T1-weighted MR image, the lesion demonstrates diffuse enhancement (arrows).

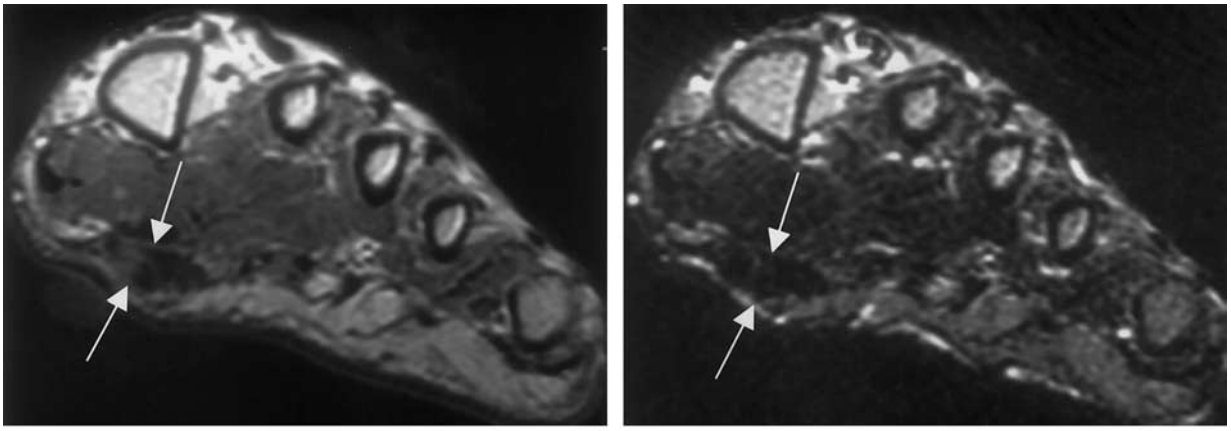

a. b.

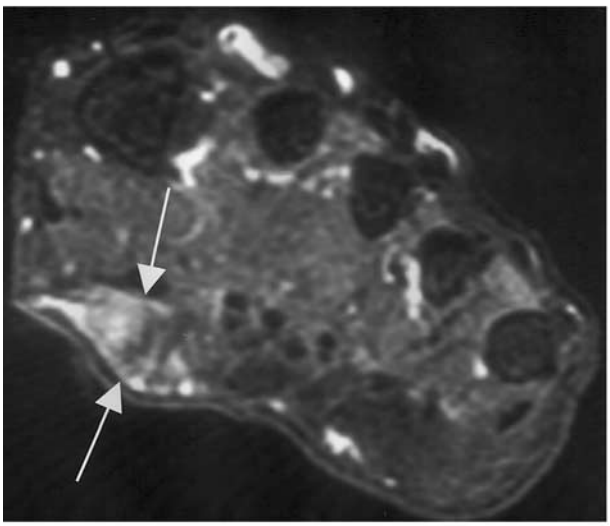

c.

Figure 17. Plantar fibromatosis in a 46-year-old man with a painful nodule in the foot. **(a)** Coronal proton-density–weighted MR image demonstrates a mass with intermediate to low signal intensity in the region of the medial plantar fascia at the proximal metatarsal level (arrows). **(b)** On a corresponding coronal T2-weighted MR image, the mass demonstrates low signal intensity (arrows). **(c)** Gadolinium-enhanced fat-suppressed T1-weighted MR image shows the lesion with marked enhancement (arrows).

a.

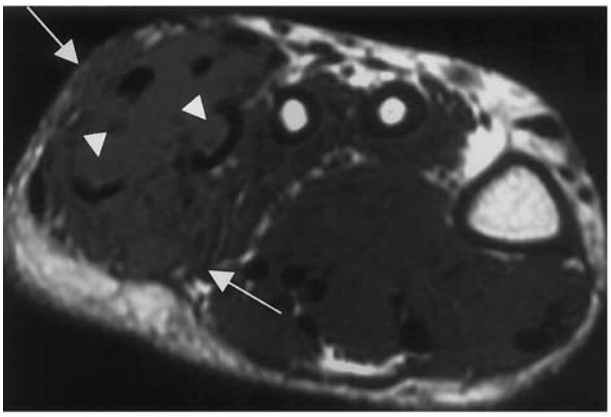

b.

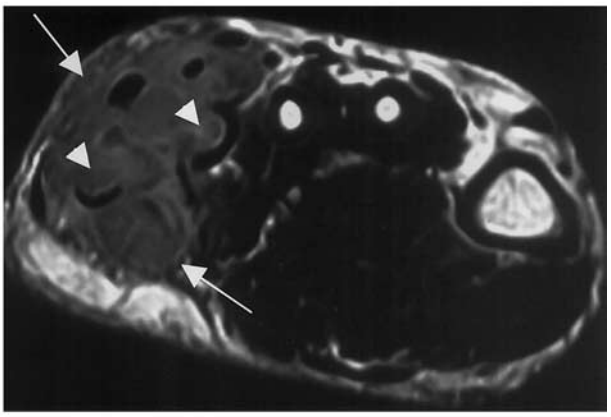

c.

Figure 18. Leiomyosarcoma in an 18-year-old woman with progressive foot pain and an enlarging mass. **(a)** Axial fat-suppressed fast spin-echo proton-density–weighted MR image reveals a predominantly high-signal-intensity mass (long arrows) invading the fifth metatarsal bone (short arrow). **(b, c)** Coronal unenhanced **(b)** and gadolinium-enhanced **(c)** T1-weighted MR images show the mass with intermediate signal intensity **(**arrows in **b)** and diffuse enhancement (arrows in **c**), respectively. Note the associated infiltration and destruction of the fourth and fifth metatarsal bones (arrowheads), a finding that indicates an aggressive tumor. This case is atypical in that leiomyosarcoma generally occurs in older individuals.

Hemangiomas

Hemangiomas typically contain areas of fat, phleboliths, and serpentine channels of high signal intensity representing dilated vascular spaces on T2-weighted images (44).

Giant Cell Tumors

Giant cell tumor of the tendon sheath is an uncommon synovial proliferative disorder characterized by low signal intensity on both T1- and T2-weighted MR images. Areas of very low signal intensity represent hemosiderin, and accentuation of these low-signal-intensity changes is characteristic with a gradient-recalled echo MR imaging sequence (52).

Soft-Tissue Neoplasms

Benign Neoplasms

Although uncommon, lipomas and nerve sheath tumors may occur in the foot. Lipomas are isointense relative to fat with all pulse sequences. Nerve sheath tumors demonstrate a nonspecific appearance. Schwannomas are well encapsulated and well defined, with intermediate signal intensity on T1-weighted MR images and increased signal intensity on T2-weighted images. Neurofibromas are not encapsulated and are often infiltrative. These neoplasms demonstrate low to intermediate signal intensity on T1-weighted images and intermediate to high signal intensity on T2-weighted images (37). Neurofibromas typically elicit pain when compression of an adjacent structure (eg, a nerve) occurs.

Malignant Neoplasms

The most common primary malignant soft-tissue neoplasm of the foot in persons under 45 years old is synovial sarcoma (44). MR imaging often reveals a heterogeneous mass with fluid levels and lobulated margins. Malignant fibrous histiosarcoma, Kaposi sarcoma, and leiomyosarcoma (Fig 18) are more common than synovial sarcoma in individuals over 45 years old (44). Symptoms generally become evident when these lesions infiltrate vital structures. Metastasis to the soft tissues of the feet is rarely described in the medical literature, although there are isolated reports of metastasis of melanoma and of breast and lung carcinoma to the superficial soft tissues (53–55).

Bone Neoplasms

Bone tumors rarely affect the feet but commonly produce pain and swelling (56,57). Bone neoplasms manifest earlier in the small bones of the feet than in the long tubular bones because the lesions do not have to become as large before producing symptoms (58). In an Armed Forces Institute of Pathology series of 255 primary bone tumors of the feet, 83.5% were benign (56). With both benign and malignant primary tumors, the metatarsal bones were most commonly affected, followed by the calcaneus. The most common benign tumor was giant cell tumor, followed by chondromyxoid fibroma and osteochondroma. The most common malignant primary bone tumors were (in decreasing order) chondrosarcoma, osteosarcoma, and Ewing sarcoma. Metastases to the bones of the feet (with the exception of the calcaneus) are rare and most frequently affect the metatarsal bones and phalanges. Lung, kidney, and colon cancer are the most common primary malignancies to metastasize to the feet (57).

MR imaging is useful for tumor detection and staging. When a bone tumor is detected at MR imaging, it is essential to correlate this finding with radiographic findings, which better suggest the histologic characteristics of the lesion.

Conclusions

MR imaging is increasingly being performed in patients who present with forefoot pain. Prior to the advent of MR imaging, many soft-tissue disorders of the metatarsal region were not diagnosed noninvasively, and the participation of radiologists in the evaluation of such patients was relatively limited. MR imaging is useful in detecting the numerous soft-tissue and early bone and joint processes that occur in this portion of the foot that are not depicted or as well characterized with other imaging modalities. Radiologists should be familiar with the differential diagnosis and MR imaging features of disorders that can produce discomfort in this area. Frequently, MR imaging allows a specific diagnosis of the condition responsible for causing metatarsal region pain.

References

1. Coughlin MJ. Conditions of the forefoot. In: Delee JC, Drez D Jr, eds. Orthopaedic sports medicine: principles and practice. Philadelphia, Pa: Saunders, 1994; 1842–2034.
2. Yao L, Do HM, Cracchiolo A, Farahani K. Plantar plate of the foot: findings on conventional arthrography and MR imaging. AJR Am J Roentgenol 1994; 163:641–644.
3. Karasick D, Schweitzer ME. Disorders of the hallux sesamoid complex: MR features. Skeletal Radiol 1998; 27:411–418.
4. Resnick D, Kang HS. Internal derangement of joints: emphasis on MR imaging. Philadelphia, Pa: Saunders, 1997.
5. Yao L, Cracciolo A, Farahani K, Seeger LL. Magnetic resonance imaging of plantar plate rupture. Foot Ankle Int 1996; 17:33–36.
6. Oloff LM, Schulhofer SD. Sesamoid complex disorders. Clin Podiatr Med 1996; 13:497–513.
7. Weinfeld SB, Haddad SL, Myerson MS. Metatarsal stress fractures. Clin Sports Med 1997; 16: 319–338.
8. Chowchuen P, Resnick D. Stress fractures of the metatarsal heads. Skeletal Radiol 1998; 27:22–25.
9. Anderson MW, Greenspan A. Stress fractures. Radiology 1996; 199:1–12.
10. Deutsch AL, Coel MN, Mink JH. Imaging of stress injuries to bone: radiography, scintigraphy and MR imaging. Clin Sports Med 1997; 16:275–290.
11. Daffner RH, Pavlov H. Stress fractures: current concepts. AJR Am J Roentgenol 1992; 159:245–252.
12. Katcherian DA. Treatment of Freiberg's disease. Orthop Clin North Am 1994; 25:69–81.
13. Morrison WB, Schweitzer ME, Batte WG, Radack DP, Russell KM. Osteomyelitis of the foot: relative importance of primary and secondary MR imaging signs. Radiology 1998; 207:625–632.
14. Gold RH, Tong DJ, Crim JR, Seeger LL. Imaging the diabetic foot. Skeletal Radiol 1995; 24:563–571.
15. Marcus CD, Ladam-Marcus VJ, Leone J, et al. MR imaging of osteomyelitis and neuropathic osteoarthropathy in the feet of diabetics. RadioGraphics 1996; 16:1337–1348.
16. Brower AC. Septic arthritis. Radiol Clin North Am 1996; 34:293–309.
17. Weishaupt D, Schweitzer ME, Alam F, Karasick D, Wapner K. MR imaging of inflammatory joint disease of the foot and ankle. Skeletal Radiol 1999; 28:663–669.
18. Yu JS. Diabetic foot and neuroarthropathy: magnetic resonance imaging evaluation. Top Magn Reson Imaging 1998; 9:295–310.
19. Wagner SC, Schweitzer ME, Morrison WB, Przybylski GJ, Parker L. Can imaging findings help differentiate spinal neuropathic arthropathy from disk space infection? initial experience. Radiology 2000; 214:693–699.
20. Tomas MB, Patel M, Marwin SE, Palestro CJ. The diabetic foot. Br J Radiol 2000; 73:443–450.
21. Karasick D, Wapner KL. Hallux rigidus deformity: radiologic assessment. AJR Am J Roentgenol 1991; 157:1029–1033.
22. Shereff MJ, Baumhauer JF. Hallux rigidus and osteoarthrosis of the first metatarsophalangeal joint. J Bone Joint Surg Am 1998; 80:898–908.
23. Schweitzer ME, Mahashwari S, Shabshin N. Hallux valgus and hallux rigidus: MRI findings. Clin Imaging 1999; 23:379–402.

24. Yu JS, Chung C, Recht M, Dailiana T, Jurdi R. MR imaging of tophaceous gout. AJR Am J Roentgenol 1997; 168:523–527.
25. Resnick D, Niwayama G. Rheumatoid arthritis. In: Resnick D, ed. Diagnosis of bone and joint disorders. 3rd ed. Philadelphia, Pa: Saunders, 1995; 866–970.
26. Beltran J, Caudill JL, Herman LA, et al. Rheumatoid arthritis: MR imaging manifestations. Radiology 1987; 165:153–157.
27. Konig H, Sieper J, Wolf KJ. Rheumatoid arthritis: evaluation of hypervascular and fibrous pannus with dynamic MR imaging enhanced with Gd-DTPA. Radiology 1990; 176:473–477.
28. Kursunoglu-Brahme S, Riccio T, Weisman MH, et al. Rheumatoid knee: role of gadopentetate-enhanced MR imaging. Radiology 1990; 176:831–835.
29. Yu JS, Popp JE, Kaeding CC, Lucas J. Correlation of MR imaging and pathologic findings in athletes undergoing surgery for chronic patellar tendinitis. AJR Am J Roentgenol 1995; 165:115–118.
30. Bencardino J, Rosenberg ZS, Defaut E. MR imaging in sports injuries of the foot and ankle. Magn Reson Imaging Clin N Am 1999; 7:131–149.
31. Mammone JF. MR imaging of tendon injuries about the foot and ankle. Clin Podiatr Med Surg 1997; 14:313–335.
32. Tehranzadeh J, Kerr R, Amster J. Magnetic resonance imaging of tendon and ligament abnormalities. II. Pelvis and lower extremities. Skeletal Radiol 1992; 21:79–86.
33. Tjin A Ton ER, Schweitzer ME, Karasick D. MR imaging of peroneal tendon disorders. AJR Am J Roentgenol 1997; 168:135–140.
34. Oloff LM, Schulhofer SD. Flexor hallucis longus dysfunction. J Foot Ankle Surg 1998; 37:101–109.
35. Glajchen N, Schweitzer ME. MRI features in de Quervain's tenosynovitis of the wrist. Skeletal Radiol 1996; 25:63–65.
36. Khoury NJ, El-Khoury GY, Saltzman CL, Brandser EA. Rupture of the anterior tibial tendon: diagnosis by MR imaging. AJR Am J Roentgenol 1996; 167:351–354.
37. Shankman S, Cisa J, Present D. Tumors of the ankle and foot. Magn Reson Imaging Clin N Am 1994; 2:139–153.
38. Morrison WB, Schweitzer ME, Wapner KL, Lackman RD. Plantar fibromatosis: a benign aggressive neoplasm with a characteristic appearance on MR images. Radiology 1994; 193:841–845.
39. Rozbruch SR, Chang V, Bohne W, Deland JT. Ganglion cysts of the lower extremity: an analysis of 54 cases and review of the literature. Orthopedics 1998; 21:141–148.
40. Ma LD, McCarthy EF, Bluemke DA, Frassica FJ. Differentiation of benign from malignant musculoskeletal lesions using MR imaging: pitfalls in MR evaluation of lesions with a cystic appearance. AJR Am J Roentgenol 1998; 170:1251–1258.
41. Bossley CJ, Cairney PC. The intermetatarsophalangeal bursa: its significance in Morton's metatarsalgia. J Bone Joint Surg Br 1980; 62:184–187.
42. Schweitzer ME, Maheshwari S, Shabshin N. Hallux valgus and hallux rigidus: MRI findings. Clin Imaging 1999; 23:397–402.
43. Zanetti M, Strehle JK, Zollinger H, Hodler J. Morton neuroma and fluid in the intermetatarsal bursae on MR images of 70 asymptomatic volunteers. Radiology 1997; 203:516–520.
44. Kransdorf MJ, Murphey MD. Imaging of soft tissue tumors. Philadelphia, Pa: Saunders, 1997.
45. Monu JU, McManus CM, Ward WG, et al. Soft-tissue masses caused by long-standing foreign bodies in the extremities: MR imaging findings. AJR Am J Roentgenol 1995; 165:395–397.
46. Varma DG, Ro JY, Guo SQ, Moulopoulos LA. Magnetic resonance imaging appearance of foreign body granulomas of the upper arms. Clin Imaging 1994; 18:39–42.
47. Fisher AR, Mason PH, Wagenhals KS. Ruptured plantar epidermal inclusion cyst. AJR Am J Roentgenol 1998; 171:1709–1710.
48. Schweitzer ME, Karasick D. MRI of the ankle and hindfoot. Semin Ultrasound CT MR 1994; 15: 410–422.
49. Zanetti M, Strehle JK, Kundert HP, Zollinger H, Hodler J. Morton neuroma: effect of MR imaging findings on diagnostic thinking and therapeutic decisions. Radiology 1999; 213:583–588.
50. Terk MR, Kwong PK, Suthar M, Horvath BC, Colleti PM. Morton neuroma: evaluation with MR imaging performed with contrast enhancement and fat suppression. Radiology 1993; 189: 239–241.
51. Erickson SJ, Canale PB, Carrera GF, et al. Interdigital (Morton) neuroma: high-resolution MR imaging with a solenoid coil. Radiology 1991; 181: 833–836.
52. Llauger J, Palmer J, Monill JM, et al. MR imaging of benign soft-tissue masses of the foot and ankle. RadioGraphics 1998; 18:1481–1498.
53. Camiel MR, Aron BS, Alexander LL, Benninghoff DL, Minkowitz S. Metastases to palm, sole, nailbed, nose, face and scalp from unsuspected carcinoma of the lung. Cancer 1969; 23:214–220.
54. Cagnoni ML, Graziani MP, Ghersetich I, et al. Multiple cutaneous melanoma metastases. Int J Dermatol 1997; 36:136–138.
55. Cohen PR, Buzdar AU. Metastatic breast carcinoma mimicking an acute paronychia of the great toe: case report and review of subungual metastases. Am J Clin Oncol 1993; 16:86–91.
56. Murari TM, Callaghan JJ, Berrey BH, Sweet DE. Primary benign and malignant osseous neoplasms of the foot. Foot Ankle Int 1989; 10:68–80.
57. Hattrup SJ, Amadio PC, Sim FH, Lombardi RM. Metastatic tumors of the foot and ankle. Foot Ankle Int 1988; 8:243–247.
58. Kricun ME. Imaging of bone tumors. Philadelphia, Pa: Saunders, 1993.

This article meets the criteria for 1.0 credit hour in category 1 of the AMA Physician's Recognition Award. To obtain credit, see accompanying test at http://www.rsna.org/education/rg_cme.html.